Acta Metall. Sin. (Engl. Lett.), 2014, **27**(4), 682–688
DOI 10.1007/s40195-014-0097-4

Effects of Annealing Temperature on the Structural, Optical, and Electrical Properties of ZnO Thin Films Grown on n-Si⟨100⟩ Substrates by the Sol–Gel Spin Coating Method

Aniruddh Bahadur Yadav · Amritanshu Pandey · S. Jit

Received: 6 October 2013 / Revised: 21 November 2013 / Published online: 11 July 2014
© The Chinese Society for Metals and Springer-Verlag Berlin Heidelberg 2014

Abstract The effects of annealing temperature on the sol–gel-derived ZnO thin films deposited on n-S⟨100⟩ substrates by sol–gel spin coating method have been studied in this paper. The structural, optical, and electrical properties of ZnO thin films annealed at 450, 550, and 650 °C in the Ar gas atmosphere have been investigated in a systematic way. The XRD analysis shows a polycrystalline nature of the films at all three annealing temperatures. Further, the crystallite size is observed to be increased with the annealing temperature, whereas the positions of various peaks in the XRD spectra are found to be red-shifted with the temperature. The surface morphology studied through the scanning electron microscopy measurements shows a uniform distribution of ZnO nanoparticles over the entire Si substrates of enhanced grain sizes with the annealing temperature. Optical properties investigated by photoluminescence spectroscopy shows an optical band gap varying in the range of 3.28–3.15 eV as annealing temperature is increased from 450 to 650 °C, respectively. The four-point probe measurement shows a decrease in resistivity from 2.1×10^{-2} to 8.1×10^{-4} Ω cm with the increased temperature from 450 to 650 °C. The study could be useful for studying the sol–gel-derived ZnO thin film-based devices for various electronic, optoelectronic, and gas sensing applications.

KEY WORDS: Nanocrystalline ZnO thin film; Sol–gel; Annealing; Surface morphology; Photoluminescence (PL); Resistivity; Grain size

1 Introduction

The environment-friendly low-cost ZnO material with direct wide band gap energy of ~3.37 eV and large exciton binding energy of ~60 meV at room temperature has drawn considerable attention in recent years for developing thin film-based nanoscaled devices for electronic [1], gas sensing [2], bio-sensing [3], piezoelectric [4], and optoelectronic [5] applications. The commonly used techniques for fabricating ZnO thin films include sputtering [6], molecular beam epitaxy [7], metal organic chemical vapor deposition (CVD) [8], spray pyrolysis [9], thermal evaporation [10], pulsed laser deposition [11], and sol–gel [12] methods. Among all the above mentioned techniques, the sol–gel is perhaps the simplest and most inexpensive synthesis technique for depositing ZnO thin films of uniform thickness over a large area of the substrates [12]. However, the sol–gel-derived ZnO films are often required to process for post-deposition heat treatment for improving the structural, optical, and electrical properties of the films.

The effect of post-deposition heat treatment temperature on various structural, optical, and electrical properties of the ZnO thin films prepared by various techniques other than the sol–gel method have been extensively studied in

Available online at http://link.springer.com/journal/40195

A. B. Yadav · A. Pandey · S. Jit (✉)
Department of Electronics Engineering, Centre for Research in Microelectronics, Indian Institute of Technology (Banaras Hindu University), Varanasi 221005, India
e-mail: sjit.ece@iitbhu.ac.in

the literature [6–11]. A number of works have also been reported on the annealing effect on the properties of sol–gel-derived ZnO films grown on various substrates including microscope glass [13], indium tin oxide (ITO) [14], sapphire [15], quartz glass [6], and Si [16] substrates. Since, ZnO is inherently an n-type semiconductor and n-Si/n-ZnO behaves as an ohmic contact [17], ZnO thin films grown on n-Si substrates could be of special interests for their compatibility with the modern day's Si-based CMOS technology. Various Schottky contacts can also be grown on the sol–gel-derived ZnO films deposited on n-Si substrates for electronic [18], optoelectronic [19], and gas sensing [20] applications. However, to the best of our knowledge, no significant research has been reported for investigating the properties of the sol–gel-derived ZnO thin films grown on n-Si substrates. Although, Xu et al. [16] reported the effect of annealing temperature on structural and optical properties of the sol–gel-derived ZnO films on Si⟨100⟩ substrates, but they did not report the type of the Si substrates (i.e., n- or p-type) used and the annealing effects on any of the electrical properties of the ZnO films. Further, their study was confined to the temperatures higher than 500 °C in air environment. In this paper, the effect of annealing temperature on various structural, electrical, and optical parameters such as the lattice constant, Zn–O bond length, grain size, stress–strain, and electrical resistivity of the sol–gel-derived ZnO thin films grown on n-Si⟨100⟩ substrates have been investigated at the 450–650 °C annealing temperatures under Argon (Ar) gas environment.

2 Experimental

Before deposition, the n-silicon (100) substrates were first cleaned in a sequence with acetone, isopropyl alcohol, and deionized (DI) water. The DI water (resistivity ~18 MΩ cm) was obtained from the Milli-Q water plant of Millipore, USA. Using diamond cutter, wafers were then cut into smaller sized samples of 2.54 cm × 2.54 cm. Zinc acetate (minimum assay ~98%, MERC) was used as the precursor for preparing the ZnO solution at the present study. The zinc acetate of 4.9 g was first dissolved in 150 mL of isopropanol and the mixture was then stirred for 35 min by magnetic stirrer at the room temperature. Once the mixture becomes milky, diethanolamine (DEA) (minimum assay ~98%, Qualingens) was added drop-wise to it (by using a 1.0 mL dropper) till a homogeneous solution is achieved. Note that DEA worked as stabilizer [12] in this case. The solution was then kept at the room temperature for 24 h for stabilization purpose. The transparent ZnO solution was deposited on n-Si (100) substrates by spin coating unit (TSE SPM 200). The rotational speed of the spin coater was fixed at 1,000 r/min for first 15 s and at

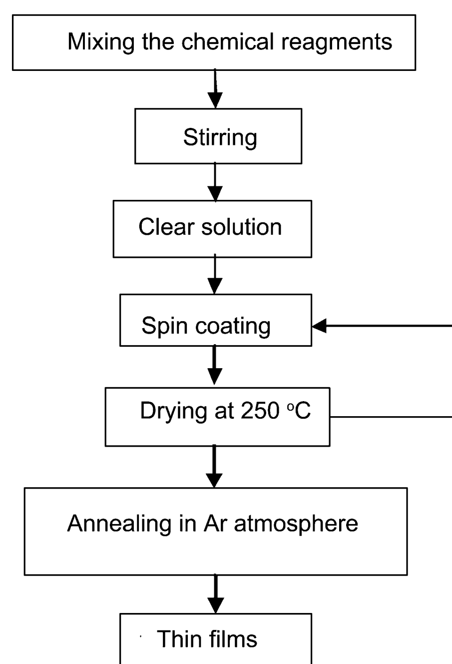

Fig. 1 Preparation steps for ZnO thin film

2,000 r/min for the next 15 s. The deposited samples were then heated for 10 min at 250 °C to remove the organic materials from the sample. The complete process of sol–gel-derived ZnO thin film by spin coating method has been depicted in the flow chart shown in Fig. 1. The process was repeated for 6 times to obtain a thickness of ~300 nm of the ZnO film. Finally, the samples were annealed in Ar atmosphere at 450, 550, and 650 °C in order to improve the crystalline structure of the film [6–16] as reported by Xue et al. [15]. The flow of Ar gas was fixed at 68.95 kPa to study only the effect of annealing temperature (at fixed flow rate of Ar) on the structural, optical, and electrical properties of the sol–gel-derived ZnO thin films considered in this paper.

The crystalline nature and phases of the as-grown ZnO film were investigated by X-ray diffraction (XRD) measurement (XRD PW-1710). The surface morphology of ZnO thin films was studied by scanning electron microscopy (SEM) (SUPRA 40 Zeiss). The optical properties were analyzed by the photoluminescence spectroscopy (PL). The electrical resistivity of the as-grown ZnO thin films was obtained by the four point probe.

It may be mentioned that the multiple coating technique was adopted in this work in the similar manner as reported in Ref. [12] where dip coating and heating were subsequently repeated for nine times. The similar methodology was also adopted in Ref. [13] where the subsequent deposition and heating processes were repeated for 8 times to obtain a ~500 nm thickness of high quality ZnO layer. In the present work, the deposition and heating in

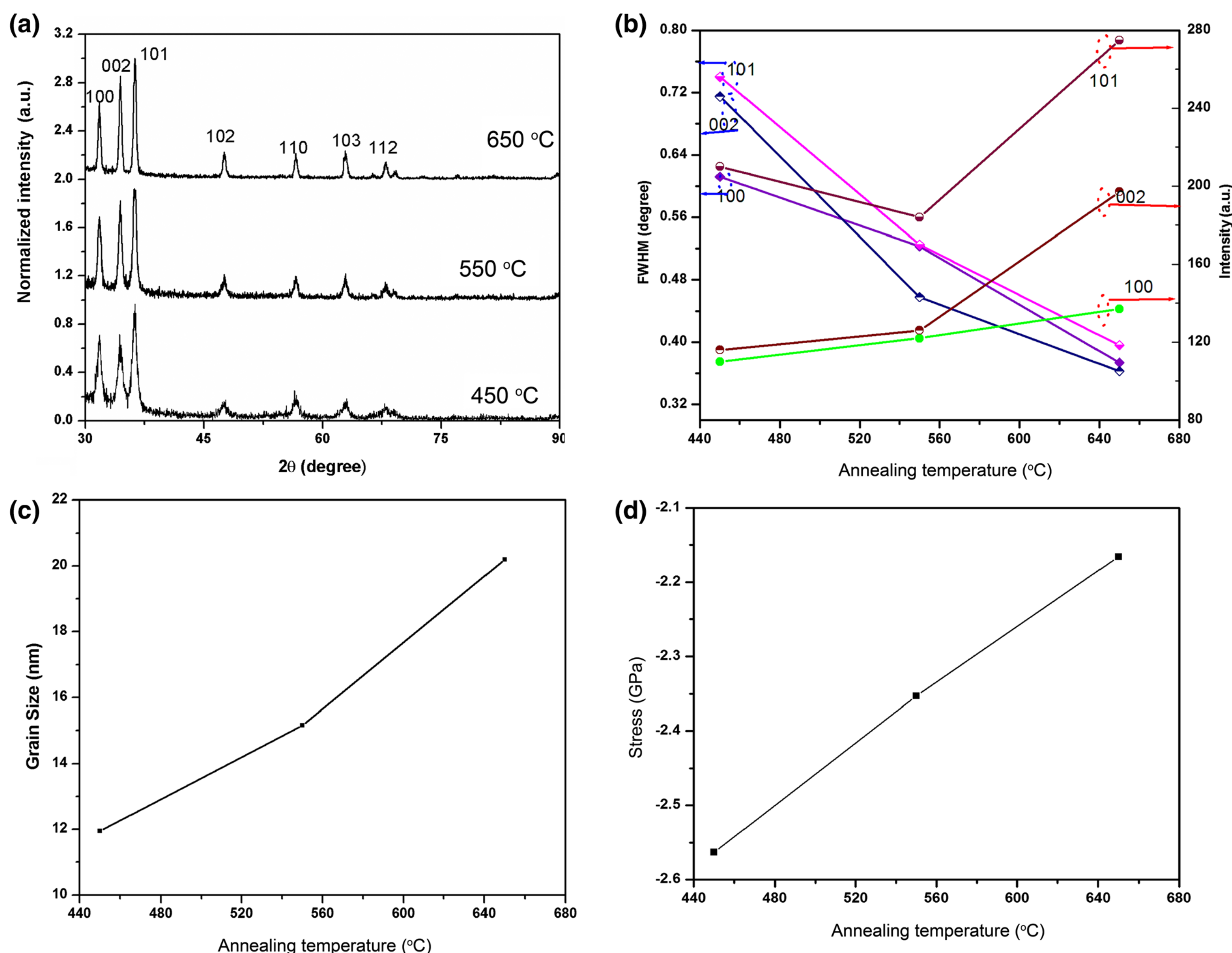

Fig. 2 XRD spectra **a**, FWHMs and peak intensities **b**, grain sizes **c**, residual stresses **d** were calculated from XRD spectra of ZnO thin film annealed in Ar atmosphere at 450–650 °C

successive manner have been repeated for 6 times to have a total film ZnO film thickness of ~300 nm. The thickness of ~300 nm was also finally verified by ellipsometric measurements. In order to maintain a uniform quality of each layer, the deposition and heating were done in nearly identical conditions which were standardized in our laboratory after verifying nearly identical SEM and XRD characteristics of each of the layers of ~50 nm thickness obtained in a single attempt of deposition by the above method.

3 Results and Discussion

3.1 Crystal Structure

Figure 2a shows the XRD analysis of the ZnO thin films grown on the n-Si (100) substrates annealed at 450, 550, and 650 °C. The sharp peaks clearly indicate that the crystalline quality of the three ZnO films is very good for all the three temperatures. According to the standard JCPDS file (No. 36-1451) [14], the peaks at 31.78°, 34.48°, 36.30°, 47.42°, 56.60°, 62.90°, and 67.87° of the film annealed at 450 °C correspond to the (100), (002), (101), (102), (110), (103), and (112) planes of ZnO crystal. The presence of these multiple peaks clearly indicates that the films are polycrystalline in nature with wurtzite hexagonal structure. Further, the most dominated peak corresponding to (101) plane is due to the use of DEA as the stabilizer during the sol–gel preparation [21]. Note that the (002) peak normally dominated over other peaks if the Monoethanolamine (MEA) is used as the stabilizer in place of the DEA [21]. The effect of annealing temperature on the full width at half maxima (FWHM) and intensities of three prominent peaks corresponding to (100), (101) and (002) planes are demonstrated in Fig. 2b. It is observed that the FWHM of the peaks is decreased, whereas the intensity is increased with the annealing temperature. The results

Table 1 Crystallite size of ZnO thin film along diffraction planes of ZnO film annealing at different temperatures

Temperature (°C)	Crystallite size (nm)			D_{moy} (nm)
	(002)	(101)	(100)	
450	14.4	9.3	12.5	11.95
550	14.5	16.3	14.7	15.16
650	19.2	21.3	20.1	20.20

Table 2 Lattice parameters, Zn–O bond length, strain, and stress for different annealing temperatures

Annealing temperature (°C)	a (nm)	c (nm)	l (nm)	Strain	Stress (MPa)
450	0.30392	0.52641	0.18734	0.0110	−2.563
550	0.30389	0.52637	0.18579	0.0101	−2.353
650	0.30341	0.52553	0.18578	0.0093	−2.166

clearly imply that the crystalline quality is improved with the annealing temperature which has also been confirmed by others [13, 14]. It may be mentioned that annealing, in general, can induce ductility, soften material, relieve internal stresses, refine the structure by making it homogeneous, and improve cold working properties. However, the relief of internal stresses in a material is a thermodynamically spontaneous process which is a very slow process at room temperatures. The annealing at high temperatures serves to accelerate the above process thereby improving the crystalline quality of the ZnO film as observed from the XRD analysis.

In order to compare the grain sizes of the ZnO nanoparticles in the films, the crystallite size is calculated by using Scherer's formula [22]:

$$D = \frac{C\lambda}{\beta\cos\theta}, \tag{1}$$

where D is the crystal size, β is the FWHM (radians), and θ is the angle of diffraction at operating wavelength $\lambda \approx 0.15405$ nm and $C \approx 0.9$ is a constant. The values of crystallite size corresponding to (100), (002), and (101) planes are summarized in Table 1 for different annealing temperatures under consideration. It is observed that the grain size (and hence crystallite size) increases with the annealing temperature. Since the increase in grain size (or crystallite size) of the nanocrystalline ZnO thin films may lead to enhance the bulk properties of the ZnO material, the crystal quality is thus improved with the increase in the grain size in the ZnO film with increasing annealing temperature. The annealing temperature effect on the average crystallite size corresponding to the (100), (002), and (101) orientation planes of the ZnO film has been shown in Fig. 2c. The increase in crystallite size with the annealing temperature in Fig. 2c implies that the surface-to-volume ratio is decreased with the annealing temperature [23].

The lattice constants a and c of the wurtzite structure of ZnO can be calculated by using the following relations [22]:

$$a = \sqrt{\frac{1}{3}}\left(\frac{\lambda}{\sin\theta}\right), \tag{2}$$

$$c = \frac{\lambda}{\sin\theta}. \tag{3}$$

The Zn–O bond length (l) for different annealing temperatures is then calculated by [24]

$$l = \sqrt{\left(\frac{a^2}{3} + \left(\frac{1}{2} - \mu\right)^2 c^2\right)}, \tag{4}$$

where μ is the positional parameter defined as [22]

$$\mu = \left(\frac{a^2}{3c^2} + 0.25\right). \tag{5}$$

The strain in the ZnO films is calculated for the different annealing temperatures by using the formula [25]:

$$\varepsilon = \frac{c_{film} - c_{bulk}}{c_{bulk}}, \tag{6}$$

where c_{film} is the lattice parameter of the ZnO thin film and c_{bulk} is the lattice parameter of the strain-free ZnO. The stress of ZnO thin film can be computed as [25]

$$\sigma = -233 \times 10^9 \left(\frac{c_{film} - c_{bulk}}{c_{bulk}}\right). \tag{7}$$

The values of all the necessary structural parameters including stress and strain present in the ZnO thin films are summarized in Table 2. The decrease in c with the increase in annealing temperature leads to the decrease in a [24]. The results imply that the ZnO thin film has built-in strain due to corresponding stress which can be relaxed by providing sufficient thermal energy to the film [16].

The variation of stress in the ZnO thin film with the annealing temperature is shown in Fig. 2d. The negative value of the stress indicates that it is of compressive in the nature [14] which is normally decreased with the annealing temperature beyond 400 °C [14, 25]. The stress is of biaxial type caused by the presence of both the intrinsic stress resulted from the intrinsic defects in the ZnO films and the extrinsic stress originated from the mismatching between the values of lattice constants and thermal coefficients of the Si-substrate and the ZnO thin films. The

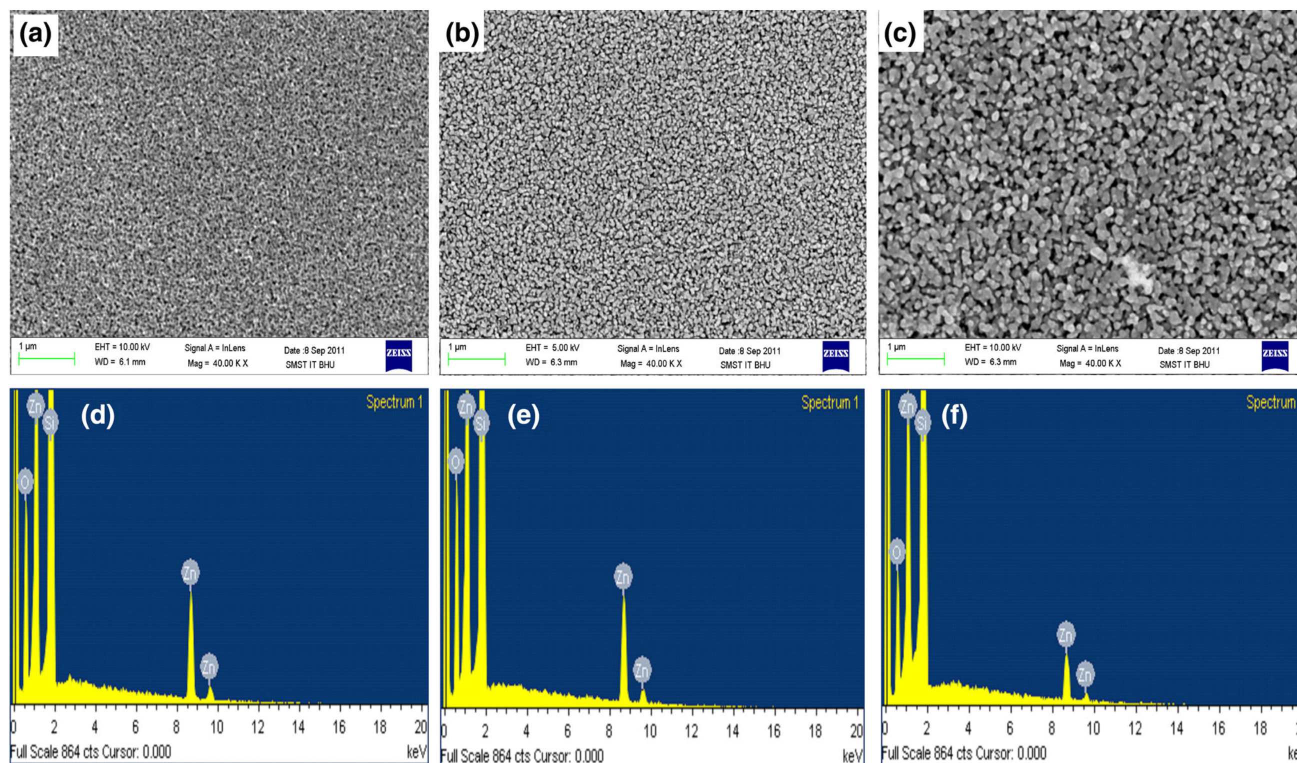

Fig. 3 SEM images and EDX resuts of ZnO thin film annealed in Ar atmosphere at different temperatures: **a**, **d** 450 °C, **b**, **e** 550 °C, **c**, **f** 650 °C

origin of the intrinsic stress may be due to crystallite imperfection in ZnO during its growth process. Several growth parameters such as deposition temperature, solution, and deposition pressure may contribute to the intrinsic stress. The decrease in the compressive stress with the annealing temperature may result in the decrease in the tensile strain in the ZnO film. The modifications in the compressive stress and tensile strain due to annealing temperature may reduce the edge emission of the ZnO in the film [24] thereby affecting the optical properties of the sol–gel-derived ZnO films considered in this paper.

3.2 Surface Morphology

The surface morphology of the as-grown ZnO thin films was studied by the SEM. The SEM images along with their respective EDX spectrum of the ZnO films annealed at 450, 550, and 650 °C have been shown in Fig. 3. Figure 3a, b, and c clearly shows a uniform deposition of ZnO nanoparticles for all the three annealing temperatures. The as-grown ZnO film is granular in nature where grain size is increased with the annealing temperature. The electron dispersive X-ray (EDX) spectra shown in Fig. 3d–f corresponding to 450, 550, and 650 °C annealing temperatures reveals only the presence of Zn and O in the as-grown ZnO films.

3.3 Analysis of Photoluminescence (PL) Characteristics

The PL spectra of the as-grown ZnO films annealed at different temperatures have been shown in Fig. 4. It is observed that, besides the main excitonic peak in the UV region, there are three very low-intensity peaks at 436.5 nm (∼2.8408 eV), 474.8 nm (∼2.6116 eV), and 525 nm (∼2.3619 eV), in the visible region whose intensities are increased at higher annealing temperatures. Further, the excitonic peak at 377 nm (∼3.2891 eV) is red-shifted to 383 nm (∼3.2376 eV) and 390 nm (∼3.1795 eV) as the annealing temperature is increased from 450 to 550 and to 650 °C, respectively. The low-intensity peak at 436.5 nm is caused by the transition of electron from the defect levels (originated from oxygen vacancies or Zn interstitials) to the valance band [16, 26]. While second low-intensity peak at 474.8 nm in the visible band may be a result of the electron transition from the shallow donor level resulting from oxygen vacancies and Zn interstitials to the valance band [16], the peak at the 525 nm normally corresponds to green emission [24].

A number of works have reported that the PL emission characteristics of ZnO thin films are strongly dependent on the crystal quality of the film [25]. The decrease in band gap energy from 3.2891 eV (∼377 nm) to 3.1795 eV

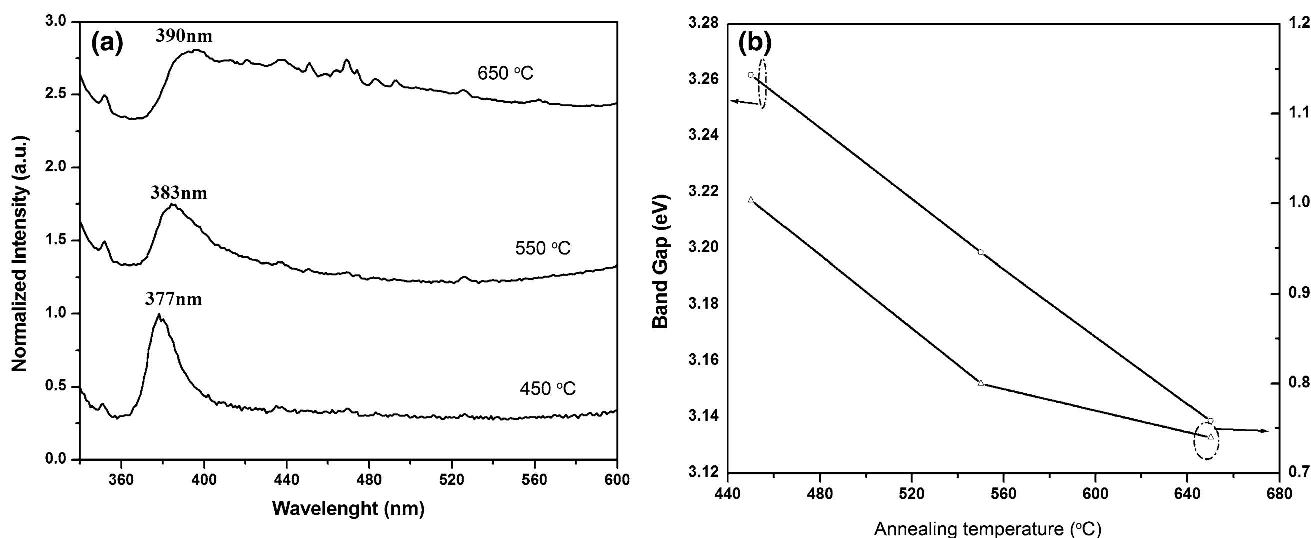

Fig. 4 Photo luminescence spectra of ZnO thin film annealed in Ar atmosphere at different temperatures **a** and the band gaps and intensities calculated from (**a**) **b**

(~390 nm) with the increased annealing temperature from 450 to 650 °C is related to the structural property of the film [16]. The larger strain due to lattice mismatching between ZnO and Si at lower annealing temperature is relaxed at elevated annealing temperatures thereby resulting in a high surface energy [14]. Further, in addition to the original growth direction of (002) plane of the ZnO, the growth in the (100) and (101) planes is enhanced with the increased annealing temperature. This results in increased defect densities including oxygen vacancies and Zn interstitials in the ZnO [25]. Thus, the reduction in the peak intensity in the UV region and enhancement in the intensity levels of the peaks in the visible region with the increased annealing temperature as observed in the PL spectra can be attributed to the enhanced defect densities as discussed above.

3.4 Annealing Temperature Effect on the Electrical Resistivity

As above, the variation of the resistivity of the sol–gel ZnO thin film as a function of the annealing temperature was presented. The sheet resistance (R_{sh}) of the n-ZnO film was measured by using a four-point probe setup. The resistivity (ρ) was calculated from the sheet resistance (R_{sh}) of the thin-film layer by using the following relationship [27]:

$$\rho = R_{sh} \times t, \tag{8}$$

$$R_{sh} = \frac{\pi}{\ln 2}\left(\frac{V}{I}\right), \tag{9}$$

where V is the voltage measured across the inner probes, I is the current applied between the outer probes, and t is the thickness of the ZnO film. Figure 5 shows the variation of the sheet resistivity (ρ) with the annealing temperature. The four probe measurement shows a decrease in the resistivity (ρ) of the sol–gel-derived ZnO thin film from $\sim 2.1 \times 10^{-2}$ to $\sim 8.1 \times 10^{-4}$ Ω cm with the increase in the annealing temperature from 450 to 650 °C, respectively. It may be observed that the resistivity of $\sim 8.1 \times 10^{-4}$ Ω cm at 650 °C appears to be very small. In this regard, it is important to mention that the ZnO thin films may possess a wide variation in the resistivity from $\sim 10^{-4}$ to $\sim 10^{8}$ Ω cm depending on the growth process conditions [28]. For example, Chen et al. [29] reported a resistivity as low as $\sim 2 \times 10^{-4}$ Ω cm of the sputtered ZnO:H films. Since resistivity is a strongly growth process-dependent parameter, the measured resistivity range of $\sim 2.1 \times 10^{-2}$ to $\sim 8.1 \times 10^{-4}$ Ω cm may be of

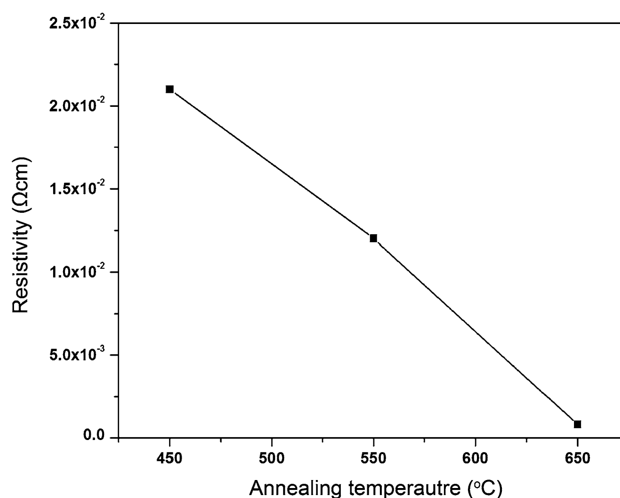

Fig. 5 Resistivity of ZnO film variation with annealing temperature

reasonable values. However, the decrease in resistivity with increasing annealing temperature may be attributed to the increase in the electron concentration due to the "grain boundary effect" as explained in Ref. [30]. At lower annealing temperatures, ZnO thin films possess a large number of smaller grains containing a large number of trapped electrons at the grain boundaries. However, as the annealing temperature is increased, many smaller sized grains are merged to form larger sized grains thereby reducing the number of grain boundaries. The electrons trapped at the smaller grain boundaries now gain enough energy to pass over the barrier of the larger sized grains. This may result in a significant increase in the free electron concentration in the ZnO films, which, in turn, may drastically reduce the resistivity of the ZnO film at higher annealing temperatures. The increase in the grain size with annealing temperature has already been discussed with reference to the analysis of the SEM and XRD results.

4 Conclusions

The effect of annealing temperature in Ar environment on some structural, electrical, and optical properties of the ZnO thin films deposited on n-Si (100) substrates by simple sol–gel method have been reported in this paper. The SEM image showed a granular nature of the ZnO film with increased grain size with the increased annealing temperature. The XRD analysis showed a polycrystalline nature of the film for all three annealing temperatures of 450, 550, and 650 °C. Various structural parameters related to lattice constants, stress and strain were estimated from the XRD results. The presence of (101) and (101) peaks in the XRD spectra was attributed to the increased defect densities of oxygen vacancies and Zn interstitial defects in ZnO film at increased annealing temperatures. The PL characteristics showed that the excitonic peak at 377 nm ($\sim$3.2891 eV) is red-shifted to 383 nm ($\sim$3.2376 eV) and 390 nm ($\sim$3.1795 eV) as the annealing temperature is increased from 450–550 to 650 °C, respectively. Three very low-intensity peaks at 436.5 nm ($\sim$2.8408 eV), 474.8 nm ($\sim$2.6116 eV), and 525 nm ($\sim$2.3619 eV) in the visible region were also observed in the PL. While the intensity of the peak in the UV was observed to be decreased with increasing annealing temperature, the intensities of the peaks in the visible region were found to be increased because of the enhancement of defect densities with the annealing temperature. The resistivity of the film estimated from the four probe measurements showed a decrease from 2.1×10^{-2} to 8.1×10^{-4} Ω cm with the increased temperature from 450 to 650 °C. The results are expected to be very useful for fabricating and characterizing sol–gel-derived ZnO thin film-based devices grown on n-Si substrates for electronic, optoelectronic, and gas sensing applications.

References

[1] R.B.M. Cross, M.M. De Souza, S.C. Deane, N.D. Young, IEEE Trans. Electron Devices **55**, 1109 (2008)
[2] P. Bhattacharyya, P.K. Basu, H. Saha, S. Basu, Sens. Actuator B **124**, 62 (2007)
[3] M. Yano, K. Koike, K.I. Ogata, T. Nogami, S. Tanabe, S. Sasa, Phys. Status Solidi C **9**, 1570 (2012)
[4] Z.C. Tu, X. Hu, Phys. Rev. B **74**, 035434 (2006)
[5] T.C. Zhang, Y. Guo, Z.X. Mei, C.Z. Gu, X.L. Dua, Appl. Phys. Lett. **94**, 113508 (2009)
[6] R.J. Hong, J.B. Huang, H.B. He, Z.X. Fan, J.D. Shao, Appl. Surf. Sci. **242**, 346 (2005)
[7] D.C. Oh, S.H. Park, H. Goto, I.H. Im, M.N. Jung, J.H. Chang, T. Yao, J.S. Song, C.H. Bae, C.S. Han, K.W. Koo, Appl. Phys. Lett. **95**, 151908 (2009)
[8] A.L. Yang, H.P. Song, D.C. Liang, H.Y. Wei, X.L. Liu, P. Jin, X.B. Qin, S.Y. Yang, Q.S. Zhu, Z.G. Wang, Appl. Phys. Lett. **96**, 151904 (2010)
[9] P. Nunes, E. Fortunato, R. Martins, Thin Solid Films **383**, 280 (2001)
[10] N. Bouhssira, S. Abed, E. Tomasella, J. Cellier, A. Mosbah, M.S. Aida, M. Jacquet, Appl. Surf. Sci. **252**, 5594 (2006)
[11] F.K. Shan, G.X. Liu, J. Korean Phys. Soc. **54**, 916 (2009)
[12] F.E. Ghodsi, H. Absalan, Acta Phys. Pol. A **118**, 659 (2011)
[13] D. Raoufi, T. Raoufi, Appl. Surf. Sci. **255**, 5812 (2009)
[14] H. Benelmadjat, S. Boudjaadar, B. Boudine, A. Chelouche, O. Halimi, A. Boudrioua, J. Optoelectron. Adv. Mater. **13**, 122 (2011)
[15] S.W. Xue, X.T. Zu, W.L. Zhou, H.X. Deng, X. Xiang, L. Zhang, H. Deng, J. Alloys Compd. **448**, 21 (2008)
[16] J.P. Xu, S.B. Shi, L. Li, X.S. Zhang, Y.X. Wang, X.M. Chen, Chin. Phys. Lett. **27**, 047803 (2010)
[17] H.Y. Kim, J.H. Kim, Y.H. Kim, K.H. Chae, C.N. Whang, J.H. Song, S. Im, Opt. Mater. **17**, 141 (2001)
[18] K. Kim, S. Kim, J. Korean Phys. Soc. **55**, 140 (2009)
[19] G.M. Ali, P. Chakrabarti, J. Vac. Sci. Technol. B **30**, 031206 (2012)
[20] J. Yu, S.J. Ippolito, W. Wlodarski, M. Strano, K. Kalantar-zade, Nanotechnology **21**, 265502 (2010)
[21] E.J. Luna-Arredondo, A. Maldonado, R. Asomoza, D.R. Acosta, M.A. Meléndez-Lira, M. de La, L. Olvera, Thin Solid Films **490**, 132 (2005)
[22] N. Shakti, P.S. Gupta, Appl. Phys. Res. **2**, 19 (2010)
[23] F. Güder, Y. Yang, J. Danhof, A. Hartel, U.T. Schwarz, M. Zacharias, Appl. Phys. Lett. **99**, 023105 (2011)
[24] G. Srinivasana, N. Gopalakrishnanc, Y.S. Yud, R. Kesavamoorthye, J. Kumara, Superlattice Microstruct. **43**, 112 (2008)
[25] A. Mahmood, N. Ahmed, Q. Raza, T. Muhammad, M. Mehmood, M.M. Hassan, N. Mahmood, Phys. Scr. **82**, 065801 (2010)
[26] X.Q. Wei, Z.G. Zhang, M. Liu, C.S. Chen, G. Sun, C.S. Xue, H.Z. Zhuang, B.Y. Man, Mater. Chem. Phys. **101**, 285 (2007)
[27] C. Periasamy, P. Chakrabarti, J. Electron. Mater. **40**, 259 (2011)
[28] Y.S. Min, C.J. An, S.K. Kim, J. Song, C.S. Hwang, Bull. Korean Chem. Soc. **31**, 2503 (2010)
[29] L.Y. Chen, W.H. Chen, J.J. Wang, F.C.N. Hong, Y.K. Su, Appl. Phys. Lett. **85**, 5628 (2004)
[30] D.H. Kim, N.G. Cho, H. Park, H.G. Kim, Integr. Ferroelectr. **95**, 35 (2007)